



# L-Arginine complex of copper on modified core–shell magnetic nanoparticles as reusable and organic–inorganic hybrid nanocatalyst for the chemoselective oxidation of organosulfur compounds

Mohsen Nikoorazm<sup>1</sup> · Parisa Moradi<sup>1</sup> · Nourolah Noori<sup>1</sup> · Gouhar Azadi<sup>1</sup>

Received: 19 January 2020 / Accepted: 14 August 2020 / Published online: 27 August 2020  
© Iranian Chemical Society 2020

## Abstract

In this paper, we report the fabrication and characterization of a stable heterogeneous nanostructure catalyst of copper immobilized on  $\text{Fe}_3\text{O}_4@ \text{SiO}_2@ \text{L-Arginine}$ , for the oxidation of sulfides and oxidative coupling of thiols. The prepared nanocatalyst has been characterized by different techniques such as FTIR, XRD, SEM, TEM and TGA. These nanoparticles were the effective catalyst for selective oxidation of sulfides and oxidative coupling of thiols using 30%  $\text{H}_2\text{O}_2$ . The suggested method offers several prominent advantages such as mild condition, use of magnetically reusable catalyst, simple workup procedure, good to high yields of products and great selectivity.

**Keywords** Magnetic nanoparticles · Copper · Oxidation reactions · Sulfide · Thiols

## Introduction

The development of noble metal nanoparticles (MNPs) has become an important subject for wide-ranging scientist and researchers. In the last decade, MNPs have reported the noteworthy potential for various applications in the field of chemical industry and catalytic process due to their strange and worthy properties, when compared to their bulk counterparts [1–5]. Generally, the surface properties of nanoparticles have to be tuned to meet the requirements for different applications.  $\text{Fe}_3\text{O}_4$  NPs are considered as ideal supports for the heterogenization of homogeneous catalysts. Metal nanoparticles (MNPs) are of significant interest for technological applications in several areas of science and industry, especially in catalysis due to their high activity [6–9]. Due to the simple and effortless separation of magnetic nanoparticles from the final products using a magnetic field, metal nanoparticles (MNPs) have been extensively studied [10–13]. Among the various metal complexes, the transition metals bearing N, O-donor ligands are a great deal of interest, and in the past decades, quantifier has been reported for different

organic transformations [14, 15]. Organic molecules are normally bounded or adsorbed onto the nanoparticle surfaces in order to design their surface properties, e.g., hydrophilicity/hydrophobicity and the availability of specific functional groups [16, 17]. Selective oxidation of sulfides to sulfoxides and oxidative coupling of thiols to disulfides is one of the consequential and most important chemical processes in both chemistry and biology [18–27]. Thus in continuation of our recent success in the development of novel and green method for the oxidation reactions [28], herein we report a simple and environmentally benign method for the selective oxidation of sulfides and oxidative coupling of thiols catalyzed by  $\text{Fe}_3\text{O}_4@ \text{SiO}_2@ \text{L-Arginine}@ \text{Cu}$ . The green nanocatalyst was easily synthesized compared with many reported procedures [29–32], and importantly, in this catalytic system L-Arginine was used as a ligand that is environmentally friendly, commercially available, inexpensive and does not use expensive and high-priced silane compounds such as 3-aminopropyltriethoxysilane or (3-chloropropyl) triethoxysilane for functionalization of catalyst.

✉ Mohsen Nikoorazm  
e\_nikoorazm@yahoo.com

<sup>1</sup> Department of Chemistry, Faculty of Science, Ilam University, P.O. Box 69315516, Ilam, Iran

## Experimental

### Materials

The reagents and materials were used in this research paper obtained from Sigma-Aldrich, Fluka or Merck chemical companies and utilized without further purification. The particles size and morphology were investigated by a JEOL JEM-2010 scanning electron microscopy (SEM), on an accelerating voltage of 200 kV. The catalyst was characterized by XRD patterns, which were collected on a Rigaku-Dmax 2500 diffractometer with nickel-filtered Cu K $\alpha$  radiation ( $\lambda = 1.5418^\circ\text{A}$ , 40 kV).

### Synthesis of the Cu immobilized on Fe<sub>3</sub>O<sub>4</sub>@SiO<sub>2</sub>@L-Arginine nanoparticles

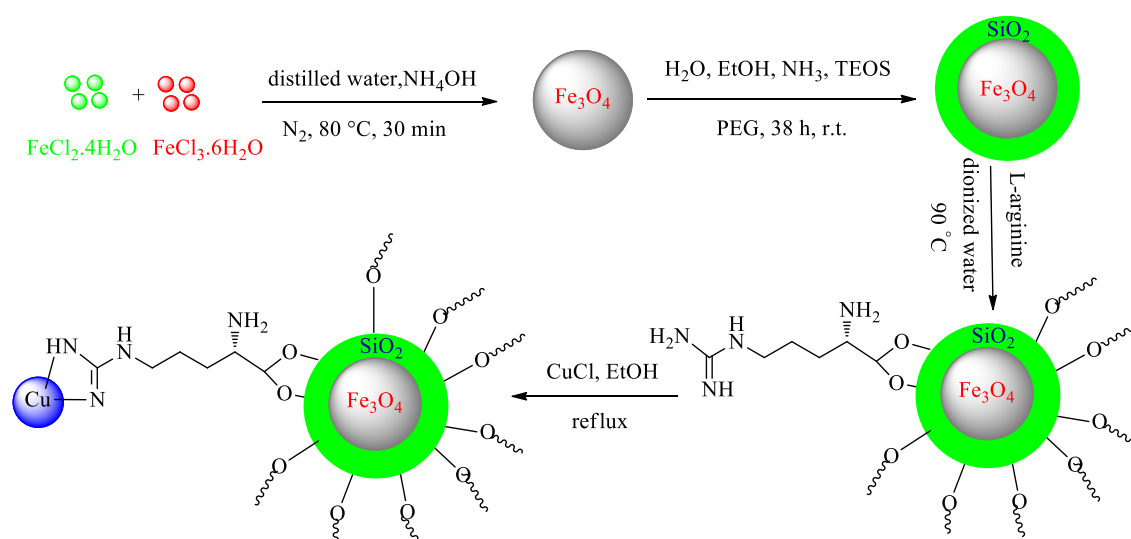
Fe<sub>3</sub>O<sub>4</sub>@SiO<sub>2</sub>@L-Arginine nanoparticles were readily synthesized similar to a previously reported work [33]. In the next step, the prepared Fe<sub>3</sub>O<sub>4</sub>@SiO<sub>2</sub>@L-Arginine (1 g) was dispersed in ethanol (50 mL) by ultrasonic bath for 30 min. Subsequently, CuCl (0.5 g) was added and the mixture was stirred at reflux conditions for 24 h. Then, the reaction mixture was cooled to room temperature and the final product was separated by a magnetic device and repeatedly washed with ethanol several times to remove the remaining impurities (Scheme 1).

### General procedure for the oxidation of sulfides to sulfoxides

To a mixture of sulfide (1 mmol), and 30% H<sub>2</sub>O<sub>2</sub> (0.5 mL), Cu immobilized on Fe<sub>3</sub>O<sub>4</sub>@SiO<sub>2</sub>@L-Arginine as catalyst (0.01 g, 8.2 mol%) was added and the mixture was stirred at room temperature in solvent-free conditions. At the end of the reaction which was monitored by TLC in the mixture of *n*-hexane and acetone (8:2), the reaction mixture was diluted with ethyl acetate and the catalyst separated using a magnetic device. Then, water (15 mL) was added to the mixture, and the product was extracted in the organic phase. The organic phase dried over anhydrous Na<sub>2</sub>SO<sub>4</sub> and then Na<sub>2</sub>SO<sub>4</sub> was removed by filtration. The filtered solvent was evaporated to give the corresponding pure sulfoxide.

### General procedure for the oxidative coupling of thiols to disulfides

A solution of thiol (1 mmol), H<sub>2</sub>O<sub>2</sub> (30%) and Cu immobilized on Fe<sub>3</sub>O<sub>4</sub>@SiO<sub>2</sub>@L-Arginine (0.005 g, 4.1 mol%) in ethyl acetate was stirred at room temperature. The reaction progress was monitored by TLC in the mixture of *n*-hexane and acetone (8:2). Then, the catalyst was separated using a magnetic field. Then, water (15 mL) was added to the reaction mixture and the product was extracted in the organic phase. Finally, the excess of solvent was removed under reduced pressure to give the corresponding pure disulfides with excellent yield.



**Scheme 1** Synthesis of Cu immobilized on Fe<sub>3</sub>O<sub>4</sub>@SiO<sub>2</sub>@L-Arginine

## Results and discussion

The catalyst synthesized using the procedure is shown in Scheme 1. Copper immobilized on  $\text{Fe}_3\text{O}_4@ \text{SiO}_2@ \text{L-Arginine}$  was fully characterized by FTIR, XRD, SEM, TGA and AAS techniques.

### Characterization of Cu immobilized on $\text{Fe}_3\text{O}_4@ \text{SiO}_2@ \text{L-Arginine}$

To understand the nature of the interaction between L-Arginine molecule and the magnetic nanoparticles, the FTIR technique was used (Fig. 1). Peaks appearing at 2924 and 2856  $\text{cm}^{-1}$  are related to the asymmetric and symmetric stretching vibrations of methylene groups ( $\text{CH}_2$ ) in all samples [34]. Stretching vibration of Fe–O and C=O bonds is presented at 583 and 1633  $\text{cm}^{-1}$ , respectively, which is confirmed that the L-Arginine was successfully supported on the magnetite surface [8]. The strong peak at 1070  $\text{cm}^{-1}$  in all spectra is related to stretching vibrations of Si–O [35]. Also, C=N stretching vibrations in the FTIR spectrum of

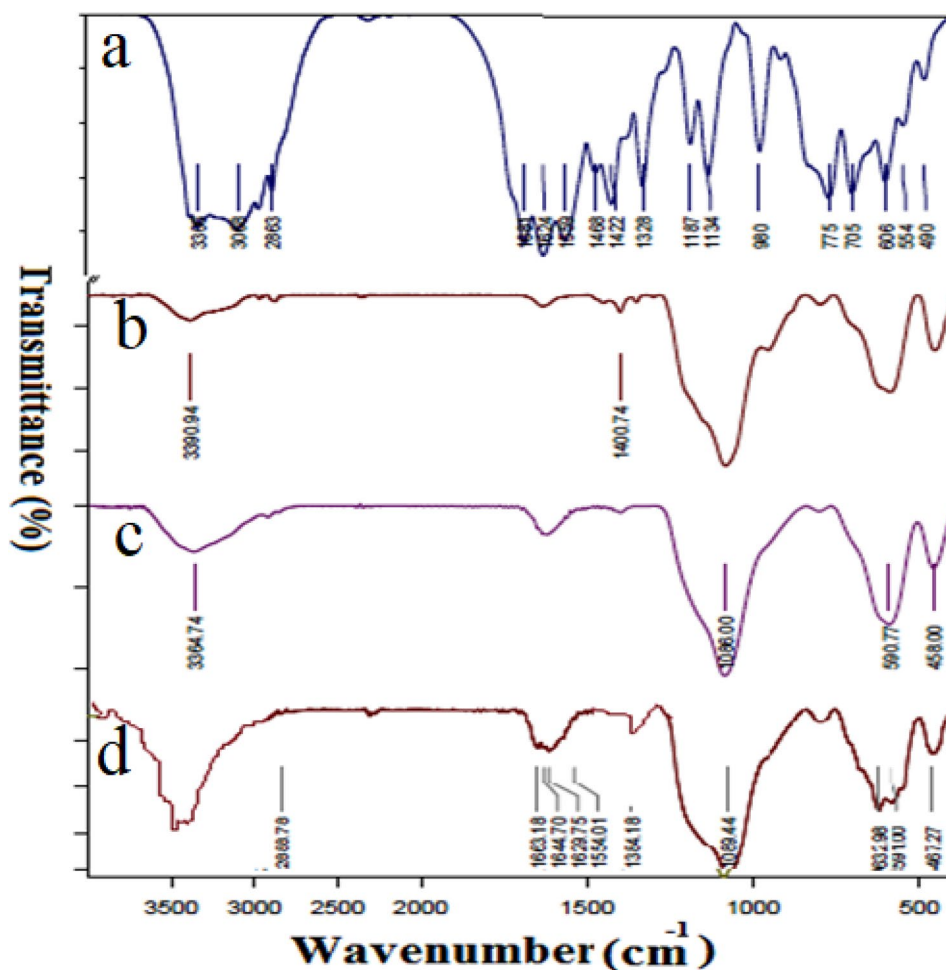
the catalyst appear at 1629  $\text{cm}^{-1}$  which is lower than C=N stretching vibrations in the FTIR spectrum of  $\text{Fe}_3\text{O}_4@ \text{SiO}_2@ \text{L-Arginine}$  due to the formation of metal–ligand bonds.

The structure and phase purity of the Cu immobilized on  $\text{Fe}_3\text{O}_4@ \text{SiO}_2@ \text{L-Arginine}$  were investigated by X-ray diffractometry (XRD). All diffraction peaks observed at  $2\theta = 30.4^\circ$ ,  $35.7^\circ$ ,  $43.2^\circ$ ,  $53.7^\circ$ ,  $57.3^\circ$  and  $63.1^\circ$  which can be assigned to the (220), (311), (400), (422), (511) and (440) planes of  $\text{Fe}_3\text{O}_4$ , respectively [36, 37]. Also, the XRD pattern of the catalyst (Fig. 2) contains a sequence of particular diffraction peaks, which are indexed to Cu indicating the presence of Cu in the prepared nanocatalyst [38, 39]. Other crystalline impurities did not show in XRD pattern, which revealed that the compositions of the catalyst are  $\text{Fe}_3\text{O}_4$  and Cu metal.

The average size of the nanocatalyst particles was calculated to be  $25 \pm 2$  nm from the XRD results by Scherrer's equation:  $D = k\lambda/\beta \cos\theta$ .

The particle size distribution of Cu immobilized on  $\text{Fe}_3\text{O}_4@ \text{SiO}_2@ \text{L-Arginine}$  was evaluated using transmission electron microscopy (TEM) (Fig. 3). This study showed

**Fig. 1** FTIR spectra of pure L-Arginine (a),  $\text{Fe}_3\text{O}_4@ \text{SiO}_2$  (b),  $\text{Fe}_3\text{O}_4@ \text{SiO}_2@ \text{L-Arginine}$  (c) and Cu immobilized on  $\text{Fe}_3\text{O}_4@ \text{SiO}_2@ \text{L-Arginine}$  (d)



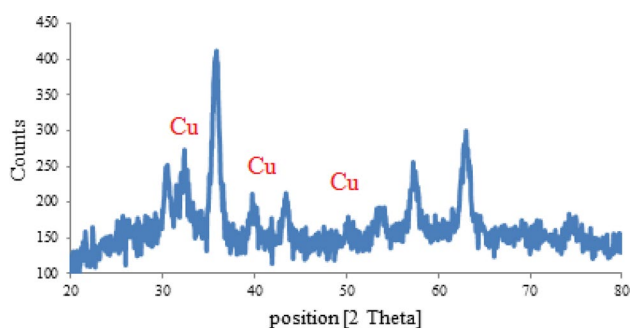


**Fig. 2** XRD pattern of the Cu immobilized on  $\text{Fe}_3\text{O}_4@SiO_2@L\text{-Arginine}$

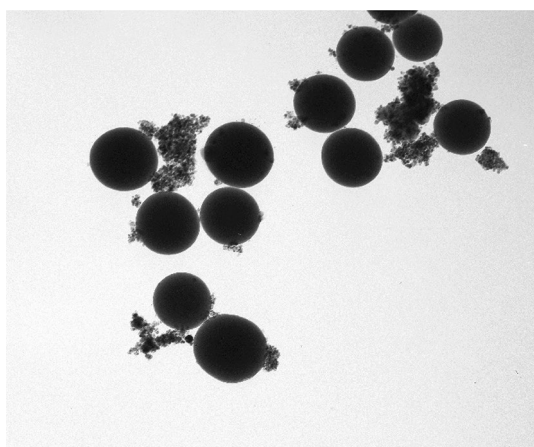


**Fig. 3** TEM images of Cu immobilized on  $\text{Fe}_3\text{O}_4@SiO_2@L\text{-Arginine}$

diameters of approximately 100–120 nm for the magnetic nanoparticles.

Selected images of scanning electron microscopy (SEM) have been used to study the structure and morphology of the catalyst. SEM images revealed that the catalyst presented the uniform particles with spherical particle morphology (Fig. 4).

The element's content of Cu immobilized on  $\text{Fe}_3\text{O}_4@SiO_2@L\text{-Arginine}$  was determined by energy-dispersive X-ray spectroscopy (EDS) analysis. The EDS diagram of this catalyst is shown in Fig. 5. As depicted, the EDS result of this catalyst shows the presence of iron, oxygen, silica, carbon, nitrogen and also copper species. X-ray mapping (WDX) is an analytical tool used to non-destructively determine the elemental analysis and chemical composition of the samples. As shown in Fig. 6, WDX analysis of Cu immobilized on  $\text{Fe}_3\text{O}_4@SiO_2@L\text{-Arginine}$  confirmed homogeneous distributions of all elements (Fe, O, Si, C, N and Cu) in the structure of this catalyst. Also, the exact amount of loaded copper chloride on  $\text{Fe}_3\text{O}_4@SiO_2@L\text{-Arginine}$  surface was also calculated by atomic absorption spectrophotometer (AAS) that was found to be  $8.2 \times 10^{-3}$  mol/g.

To indicate the bond formation between the  $\text{Fe}_3\text{O}_4$  MNPs with the organic spacer group and to obtain information on the thermal stability, the thermogravimetric analysis (TGA) was performed (Fig. 7). The TGA/DTA/DTG diagrams of Cu immobilized on  $\text{Fe}_3\text{O}_4@SiO_2@L\text{-Arginine}$  are shown three mass loss over the temperature range of 27–800 °C by heating rates at 10 °C/min and in the air atmosphere. The weight loss of ~5% in the

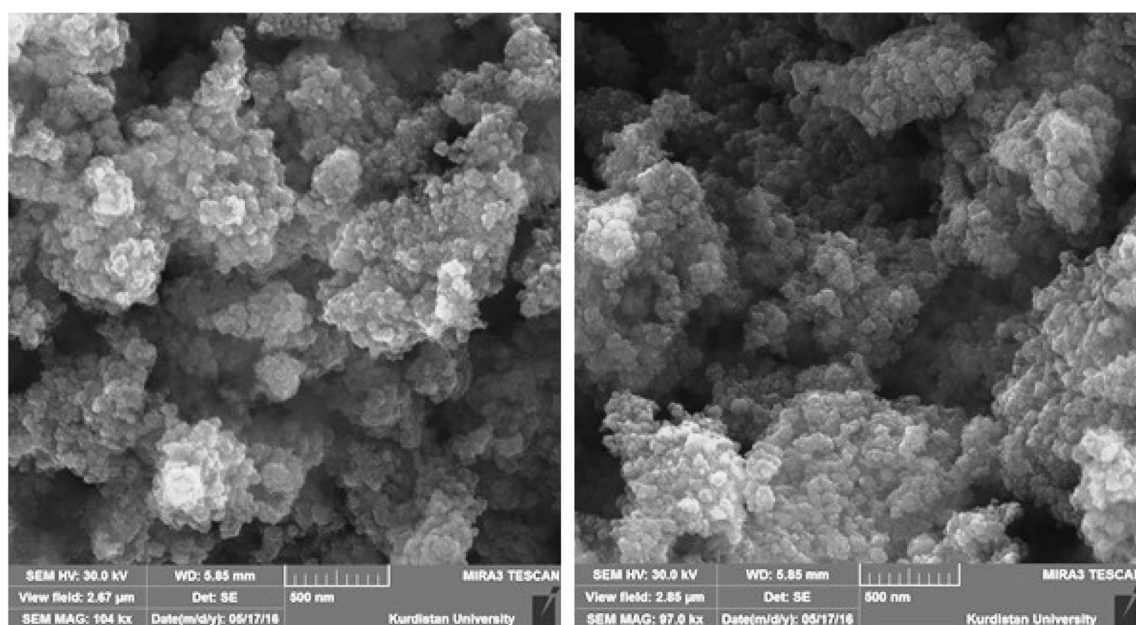


**Fig. 4** SEM images of the Cu immobilized on  $\text{Fe}_3\text{O}_4@SiO_2@L\text{-Arginine}$



**Fig. 5** EDS diagram of Cu immobilized on  $\text{Fe}_3\text{O}_4@$   $\text{SiO}_2@$ L-Arginine

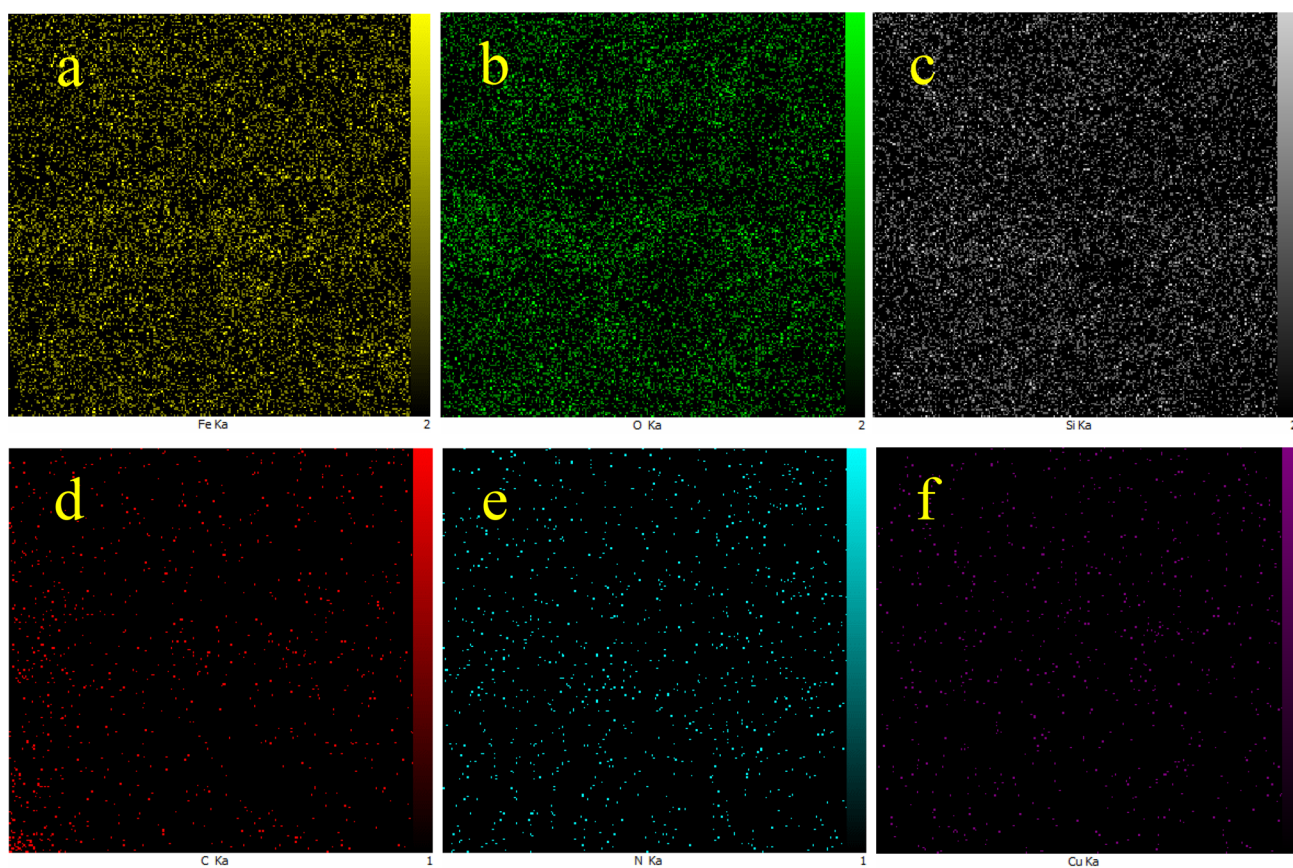
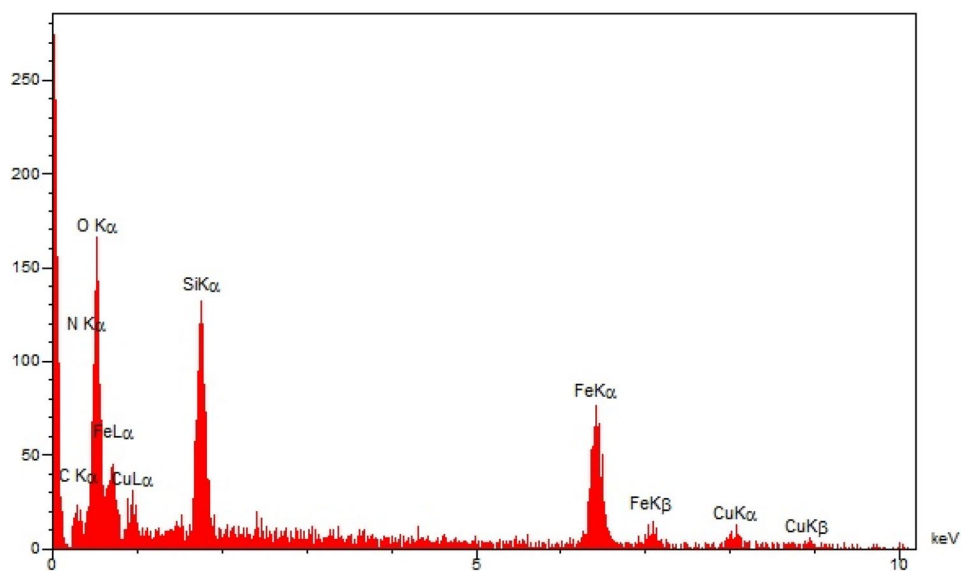
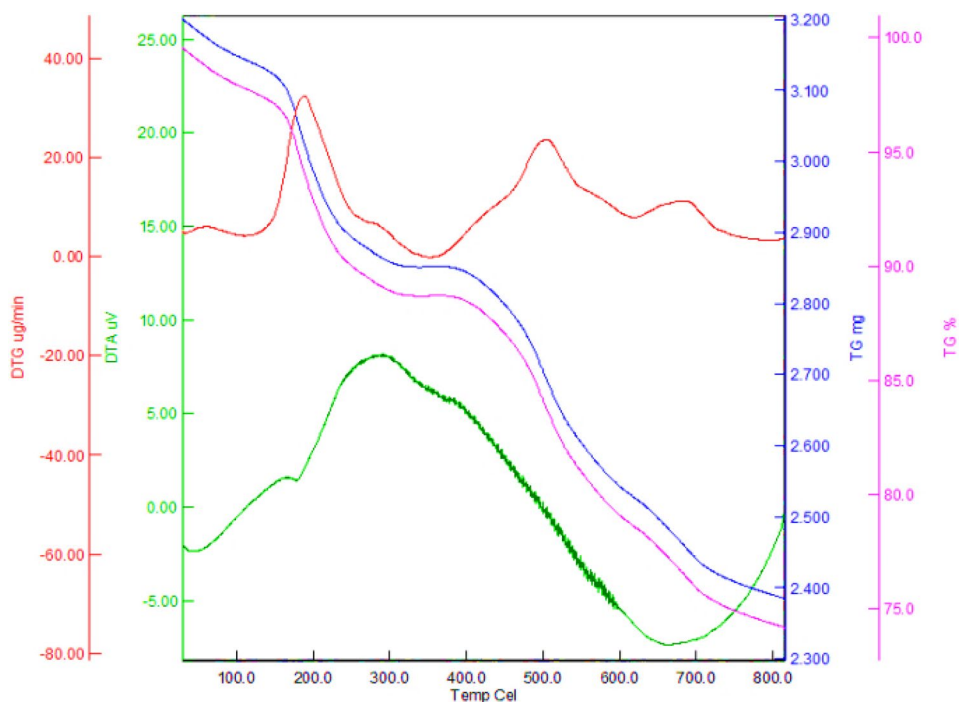


**Fig. 6** Elemental mapping of **a** Fe, **b** O, **c** Si, **d** C, **e** N and **f** Cu for Ni-Cytosine@MCM-41

temperature range of 100–250 °C attributed to the removal of physically adsorbed solvent and water [40, 41]. Besides, the analysis showed another decreasing peak at a temperature between 250 and 600 °C due to the decomposition of

the organic spacer group [42, 43]. The final weight loss (about 2%) indicated above 600 °C which is corresponded to the condensation of the silanol groups [40, 44].

**Fig. 7** TGA/DTA/DTG analysis of Cu immobilized on Fe<sub>3</sub>O<sub>4</sub>@SiO<sub>2</sub>@L-Arginine



## Catalytic study

The oxidation of sulfides and oxidative coupling of thiols are the most important functional group transformations in organic synthesis, as they are highly useful intermediates and building blocks in the preparation of numerous chemically and biologically active compounds. Thus, these reactions were considered to study the catalytic activity of the prepared catalyst. In order to optimize the reaction condition, the oxidation reaction of methyl phenyl sulfide and

2-mercaptobenzoxazole (Scheme 2) has been selected as model reactions. Initially, the reactions were performed in different solvents, which the results indicated solvent-free conditions and ethyl acetate were preferable mediums for the oxidation of sulfides and oxidative coupling of thiols, respectively (Table 1, entries 4, 7). Then, the reaction was evaluated by different amounts of catalyst. As can be seen from Table 1, the yield of products and the rate of the reaction were also found to be dependent on the concentration of the catalyst. Therefore, 0.01 g of catalyst for oxidation of

**Table 1** Oxidation reactions of methyl phenyl sulfide and 2-mercaptobenzoxazole in the presence of Cu immobilized on Fe<sub>3</sub>O<sub>4</sub>@SiO<sub>2</sub>@L-Arginine

Entry	Substrate	Solvent	Catalyst (mg)	Time (min)	Yield (%) <sup>a</sup>
1	Methyl phenyl sulfide	EtOH	10	120	N.R.
2	Methyl phenyl sulfide	CH <sub>3</sub> CN	10	120	N.R.
3	Methyl phenyl sulfide	EtOAc	10	120	N.R.
4	Methyl phenyl sulfide	Solvent free	10	120	96
5	Methyl phenyl sulfide	Solvent free	8	120	90
6	Methyl phenyl sulfide	Solvent free	5	120	80
7	2-Mercaptobenzoxazole	EtOAc	5	30	98
8	2-Mercaptobenzoxazole	EtOAc	3	30	81
9	2-Mercaptobenzoxazole	EtOAc	2	30	65
10	2-Mercaptobenzoxazole	Solvent free	5	30	60
11	2-Mercaptobenzoxazole	EtOH	5	30	89
12	2-Mercaptobenzoxazole	CH <sub>3</sub> CN	5	30	80
13	2-Mercaptobenzoxazole	CH <sub>2</sub> Cl <sub>2</sub>	5	30	54
14	2-Mercaptobenzoxazole	Acetone	5	30	70

Reaction condition: sulfide or thiol (1 mmol), H<sub>2</sub>O<sub>2</sub> 30% (0.5 mL), solvent (5 mL), room temperature

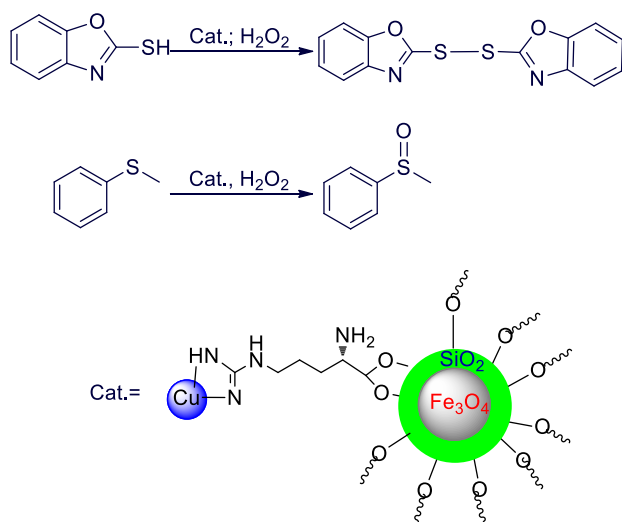
<sup>a</sup>Isolated yield

sulfides and 0.005 g of catalyst for oxidation of thiols were found to be optimum amounts at room temperature, respectively (Table 1, entries 4, 7).

Then, we have extended the procedure using structurally diverse sulfides and thiols under optimized reaction conditions (Scheme 3). As shown in Table 2, all the examined substrates obtained the corresponding products in good to excellent yields compared with many reported procedures and the catalytic systems performed in a green medium. This catalyst is shown a good selectivity for the oxidation of sulfides to sulfoxides without overoxidation to formation of sulfone as by-product. More importantly, this catalytic system is chemoselective. When we used the substrates including COOCH<sub>3</sub>, OH, COOH and carbon–carbon double bond functional groups, these substrates selectively underwent oxidation at the sulfur atom without extra structural changes in their functional group that is an attractive feature of these catalytic systems (Scheme 4).

### Catalyst recovery

The most important advantage of the applied catalyst is recoverability and reusability. It is important to note that the magnetic property of this catalyst facilitates its efficient recovery from the final products. In this regard, the reusability of the nanostructure catalysts for subsequent catalytic cycles was examined using dipropyl sulfide and 2-mercaptobenzoxazole as the substrate. To recover the catalyst after completion of the reaction, the catalyst was isolated by applying an external magnetic field and then washed with acetone to remove residual product and dried at vacuum. Then, the reaction vessel was charged with the



**Scheme 2** Oxidation of methyl phenyl sulfide and 2-mercaptobenzoxazole in the presence of Cu immobilized on Fe<sub>3</sub>O<sub>4</sub>@SiO<sub>2</sub>@L-Arginine

fresh substrate and subjected to the next. As shown in Fig. 8, the change in the product yield was negligible in a trial of five recycling experiments, which demonstrates the practical recyclability of this catalyst. The atomic absorption technique was used to determine the amount of copper leaching after recovery. Thus, using the atomic absorption technique, the amount of copper found in the final catalyst was measured. It was found that the amount of copper before the reaction was  $8.2 \times 10^{-3}$  mol/g and after the reaction became  $7.9 \times 10^{-3}$  mol/g, indicating a very slight and measurable change in the amount of copper during the reaction that indicates the heterogeneity of the catalytic reaction.

To consider the heterogeneity of catalyst, the catalyst was separated by applying a magnetic field after half of the normal reaction time in the oxidation of methyl phenyl sulfide. The filtrate was then allowed to react further as normal. After catalyst separation, the progress of the reaction was increased only 5%, which shows the heterogeneity of this catalytic system.

The XRD pattern of the recovered catalyst (Fig. 9) includes several peaks which are indexed to copper and Fe<sub>3</sub>O<sub>4</sub> nanoparticles. The XRD pattern of the recovered catalyst is shown good agreement with fresh catalyst. As shown in Fig. 9, the XRD pattern of recovered catalyst showed a good stability of the catalyst after recycling.

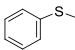
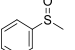
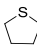
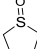
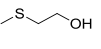
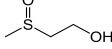
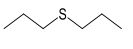
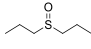
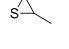
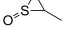
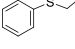
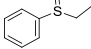
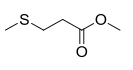
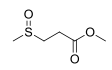
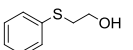
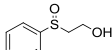
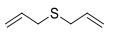
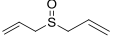
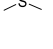
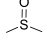
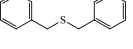
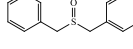
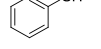
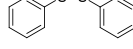
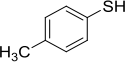
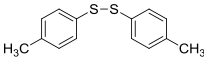
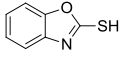
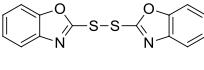
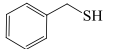
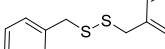
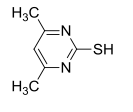
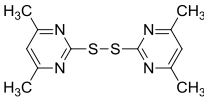
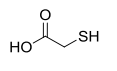
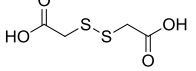
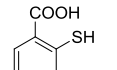
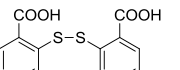
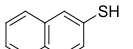
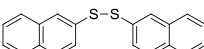
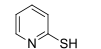
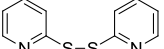
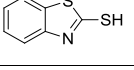
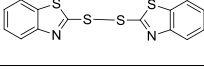
### Comparison of the catalysts

To establish the high catalytic activity of the synthesized catalyst and greenness of this method, we compared our results on the oxidation of methyl phenyl sulfide and oxidative coupling of 4-methylbenzenethiol with data from the literature (Table 1). As can be seen from Table 3, this catalytic system is greener. More importantly at the end of the reaction, the catalyst was easily separated using an external magnet and does not need any filtration.

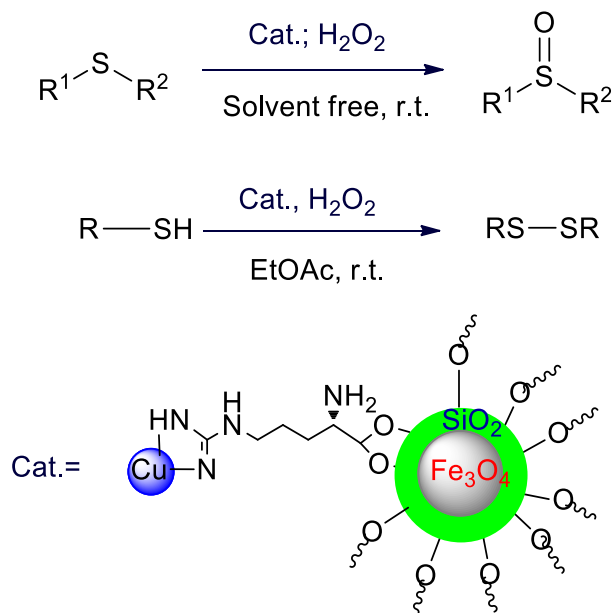
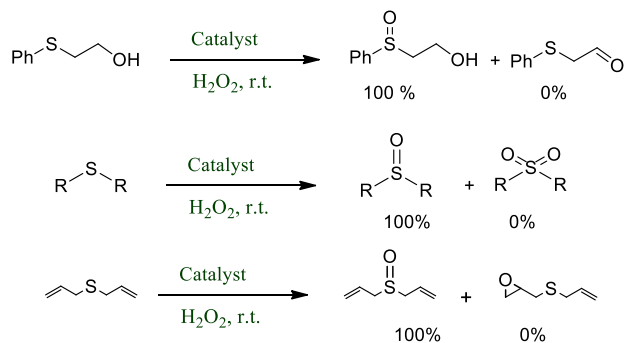
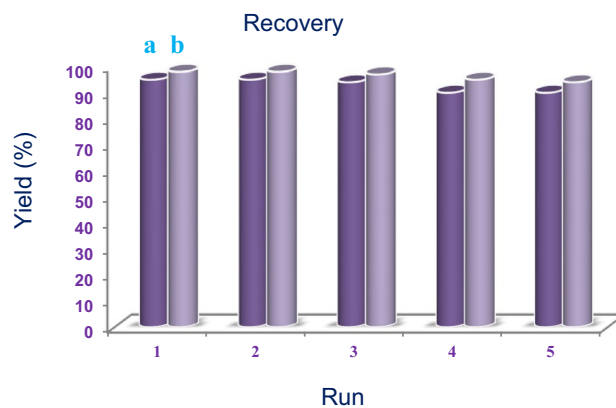
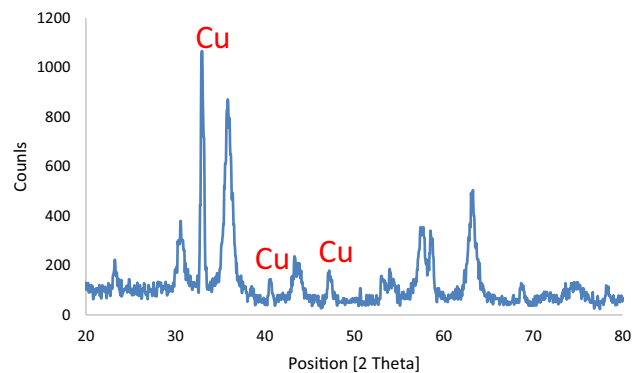
### Conclusion

In conclusion, we introduced a simple method for the synthesis of Cu immobilized on Fe<sub>3</sub>O<sub>4</sub>@SiO<sub>2</sub>@L-Arginine as heterogeneous nanostructure catalyst. The catalyst was applied for the oxidation of sulfides and oxidative coupling of thiols. The prominent features of this method are the use of non-toxic, commercially available, inexpensive and green substrate for the synthesis of catalyst, simple experimental procedure, applicability to various substrates, waste-free, green and efficient synthetic entry to excellent yield. Furthermore, nanocatalyst can be easily recovered by a magnetic field and reused for subsequent reactions with high generation efficiency.

**Table 2** Oxidation of sulfides and oxidative coupling of thiols in the presence of Cu immobilized on Fe<sub>3</sub>O<sub>4</sub>@SiO<sub>2</sub>@L-Arginine

Entry	Substrate	Product	Time (min)	Yield <sup>a</sup> (%)
1			120	96
2			5	90
3			2	95
4			45	95
5			1	92
6			200	95
7			10	98
8			30	95
9			30	91
10			30	90
11			180	85
12			15	97
13			12	95
14			30	98
15			80	96
16			60	94
17			15	95
18			75	65
19			90	70
20			25	98
21			45	97



**Table 2** (continued)Reaction condition for oxidation of sulfides/H<sub>2</sub>O<sub>2</sub>/Cat. (1 mmol:0.5 mL:10 mg) and thiols/H<sub>2</sub>O<sub>2</sub>/Cat. (1 mmol:0.5 mL:5 mg)<sup>b</sup>Isolated product**Scheme 3** Oxidation of sulfides and oxidative coupling of thiols in the presence of Cu immobilized on Fe<sub>3</sub>O<sub>4</sub>@SiO<sub>2</sub>@L-Arginine**Scheme 4** Chemoselective sulfoxidation of sulfides in the presence of Cu immobilized on Fe<sub>3</sub>O<sub>4</sub>@SiO<sub>2</sub>@L-Arginine**Fig. 8** The recycling experiment of Cu immobilized on Fe<sub>3</sub>O<sub>4</sub>@SiO<sub>2</sub>@L-Arginine in the oxidation reaction of dipropyl sulfide (column a) and 2-mercaptobenzoxazole (column b)**Fig. 9** XRD pattern of the recovered Cu immobilized on Fe<sub>3</sub>O<sub>4</sub>@SiO<sub>2</sub>@L-Arginine

**Table 3** Comparison of  $\text{Fe}_3\text{O}_4@\text{SiO}_2@\text{L-Arginine}$  with other reported catalysts for oxidation of methyl phenyl sulfide and oxidative coupling of 4-methylbenzenethiol

Entry	Substrate	Catalyst	Time (h)	Yield (%)
1	Methyl phenyl sulfide	$\text{VO}_2\text{F}(\text{dmpz})_2$	5	95 [45]
2	Methyl phenyl sulfide	$\text{ZnBr}_2$	6	85 [46]
3	Methyl phenyl sulfide	SSA	0.5	92 [47]
4	Methyl phenyl sulfide	Zr-oxide@MCM-41	6	98 [48]
5	Methyl phenyl sulfide	Polymer-anchored Cu(II)	3	90 [49]
6	Methyl phenyl sulfide	NBS	4.5	93 [50]
7	Methyl phenyl sulfide	$\text{Nb}_2\text{O}_5/\text{AC}$	2	93.4 [51]
8	Methyl phenyl sulfide	$[\text{VO}(\text{TPPABr})]\text{CBr}_3$	2	93 [52]
9	4-Methylbenzenethiol	Zr-oxide@MCM-41	0.5	99 [48]
10	4-Methylbenzenethiol	Silica sulfuric acid	1.7	98 [53]
11	4-Methylbenzenethiol	Zr(IV)-ninhydrin supported MCM-41	2	98 [54]
12	4-Methylbenzenethiol	Zr(IV)-ninhydrin supported MCM-48	3	98 [54]
13	4-Methylbenzenethiol	Ni-salen-MCM-41	0.42	95 [55]
14	4-methylbenzenethiol	Cd-salen-MCM-41	0.33	97 [55]
15	4-Methylbenzenethiol	$\text{Fe}_3\text{O}_4@\text{SiO}_2@\text{L-Arginine}$	0.2	95 [this work]
16	Methyl phenyl sulfide	$\text{Fe}_3\text{O}_4@\text{SiO}_2@\text{L-Arginine}$	2	96 [this work]

**Acknowledgements** This work was supported by the research facilities of Ilam University, Ilam, Iran.

## References

- S. Gao, N. Koshizaki, H. Tokuhisa, E. Koyama, T. Sasaki, J.K. Kim, J. Ryu, D.S. Kim, Y. Shimizu, Highly stable Au nanoparticles with tunable spacing and their potential application in surface plasmon resonance biosensors. *Adv. Func. Mater.* **20**, 78–86 (2010). <https://doi.org/10.1002/adfm.200901232>
- T.K. Sau, A.L. Rogach, F. Jäckel, T.A. Klar, J. Feldmann, Properties and applications of colloidal nonspherical noble metal nanoparticles. *Adv. Mater.* **22**, 1805–1825 (2010). <https://doi.org/10.1002/adma.200902557>
- D.Y. Wu, X.M. Liu, Y.F. Huang, B. Ren, X. Xu, Z.Q. Tian, Surface catalytic coupling reaction of p-mercaptoaniline linking to silver nanostructures responsible for abnormal SERS enhancement: a DFT study. *J. Phys. Chem. C* **113**, 18212–18222 (2009). <https://doi.org/10.1021/jp9050929>
- S. Li, S.R. Zhai, Q.D. An, M.H. Li, Y. Song, X.W. Song, Designed synthesis of multifunctional  $\text{Fe}_3\text{O}_4@\text{SiO}_2\text{-NH}_2@\text{CS-Co(II)}$  towards efficient oxidation of ethylbenzene. *Mater. Res. Bull.* **60**, 665–673 (2014). <https://doi.org/10.1016/j.materresbull.2014.09.042>
- J. Zhang, S. Zhai, S. Li, Z. Xiao, Y. Song, Q. An, G. Tian, Pb(II) removal of  $\text{Fe}_3\text{O}_4@\text{SiO}_2\text{-NH}_2$  core-shell nanomaterials prepared via a controllable sol-gel process. *Chem. Eng. J.* **215**, 461–471 (2013). <https://doi.org/10.1016/j.cej.2012.11.043>
- Y. Chen, F. Zhang, Y. Fang, X. Zhu, W. Zhen, R. Wang, J. Ma, Phosphotungstic acid containing ionic liquid immobilized on magnetic mesoporous silica rod catalyst for the oxidation of dibenzothiophene with  $\text{H}_2\text{O}_2$ . *Catal. Commun.* **38**, 54–58 (2013). <https://doi.org/10.1016/j.catcom.2013.04.005>
- Y. Jiang, C. Guo, H. Xia, I. Mahmood, C. Liu, H. Liu, Magnetic nanoparticles supported ionic liquids for lipase immobilization: enzyme activity in catalyzing esterification. *J. Mol. Catal. Enzym.* **58**, 103–109 (2009). <https://doi.org/10.1016/j.molcatb.2008.12.001>
- V. Polshettiwar, R. Luque, A. Fihri, H. Zhu, M. Bouhrara, J.M. Basset, Magnetically recoverable nanocatalysts. *Chem. Rev.* **111**, 3036–3075 (2011). <https://doi.org/10.1021/cr100230z>
- J. Wang, B. Xu, H. Sun, G. Song, Palladium nanoparticles supported on functional ionic liquid modified magnetic nanoparticles as recyclable catalyst for room temperature Suzuki reaction. *Tetrahedron Lett.* **54**, 238–241 (2013). <https://doi.org/10.1016/j.tetlet.2012.11.009>
- B. Tahmasbi, A. Ghorbani-Choghamarani, Magnetic MCM-41 nanoparticles as a support for the immobilization of a palladium organometallic catalyst and its application in C–C coupling reactions. *New J. Chem.* **43**, 14485–14501 (2019). <https://doi.org/10.1039/C9NJ02727K>
- M. Esmaeilpour, A.R. Sardarian, J. Javidi, Schiff base complex of metal ions supported on superparamagnetic  $\text{Fe}_3\text{O}_4@\text{SiO}_2$  nanoparticles: an efficient, selective and recyclable catalyst for synthesis of 1,1-diacetates from aldehydes under solvent-free conditions. *Appl. Catal. A Gen.* **445**, 359–367 (2012). <https://doi.org/10.1016/j.apcata.2012.09.010>
- A. Ghorbani-Choghamarani, B. Tahmasbi, N. Noori, S. Faryadi, Pd–S-methylisothiourrea supported on magnetic nanoparticles as an efficient and reusable nanocatalyst for Heck and Suzuki reactions. *C. R. Chim.* **20**, 132–139 (2017). <https://doi.org/10.1016/j.crci.2016.06.010>
- N.T. Phan, H.V. Le, Superparamagnetic nanoparticles-supported phosphine-free palladium catalyst for the Sonogashira coupling reaction. *J. Mol. Catal. A: Chem.* **334**, 130–138 (2011). <https://doi.org/10.1016/j.molcata.2010.11.009>
- J. Andrez, G. Bozoklu, G. Nocton, J. Pecaute, R. Scopelliti, L. Dubois, M. Mazzanti, Lanthanide(II) complexes supported by N,O-donor tripodal ligands: synthesis, structure, and ligand-dependent redox behavior. *Chem. Eur. J.* **21**, 15188–15200 (2015). <https://doi.org/10.1002/chem.201502204>
- R.N. Baig, R.S. Varma, Organic synthesis via magnetic attraction: benign and sustainable protocols using magnetic nanoferrites. *Green Chem.* **15**, 398–417 (2013). <https://doi.org/10.1039/C2GC36455G>
- K. Azizi, M. Karimi, H.R. Shaterian, A. Heydari, Ultrasound irradiation for the green synthesis of chromenes using L-arginine-functionalized magnetic nanoparticles as a recyclable

- organocatalyst. *RSC Adv.* **4**, 42220–42225 (2014). <https://doi.org/10.1039/C4RA06198E>
17. M. Nasr-Esfahani, S.J. Hoseini, M. Montazerzohori, R. Mehrabi, H. Nasrabadi, Magnetic Fe<sub>3</sub>O<sub>4</sub> nanoparticles: efficient and recoverable nanocatalyst for the synthesis of polyhydroquinolines and Hantzsch 1,4-dihydropyridines under solvent-free conditions. *J. Mol. Catal. A: Chem.* **382**, 99–105 (2014). <https://doi.org/10.1016/j.molcata.2013.11.010>
  18. A. Ghorbani-Choghamarani, P. Moradi, B. Tahmasbi, Nickel(II) immobilized on dithizone–boehmite nanoparticles: as a highly efficient and recyclable nanocatalyst for the synthesis of polyhydroquinolines and sulfoxidation reaction. *J. Iran. Chem. Soc.* **16**, 511–521 (2019). <https://doi.org/10.1007/s13738-018-1526-5>
  19. A. Akdag, T. Webb, S. Worley, Oxidation of thiols to disulfides with monochloro poly(styrenehydantoin) beads. *Tetrahedron Lett.* **47**, 3509–3510 (2006). <https://doi.org/10.1016/j.tetlet.2006.03.105>
  20. S. Kumar, S. Verma, S.L. Jain, B. Sain, Thiourea dioxide (TUD): a robust organocatalyst for oxidation of sulfides to sulfoxides with TBHP under mild reaction conditions. *Tetrahedron Lett.* **52**, 3393–3396 (2011). <https://doi.org/10.1016/j.tetlet.2011.04.088>
  21. B. Li, A.H. Liu, L.N. He, Z.Z. Yang, J. Gao, K.H. Chen, Iron-catalyzed selective oxidation of sulfides to sulfoxides with the polyethylene glycol/O<sub>2</sub> system. *Green Chem.* **14**, 130–135 (2012). <https://doi.org/10.1039/C1GC15821J>
  22. R. Ozen, F. Aydin, Oxidation of thiols to disulfides with molecular oxygen in subcritical water. *Monatsh. Chem. Mon. Monatsh. Chem.* **137**, 307–310 (2006). <https://doi.org/10.1007/s00706-005-0430-8>
  23. S. Samanta, S. Ray, A.B. Ghosh, P. Biswas, 3,6-Di(pyridin-2-yl)-1,2,4,5-tetrazine (pytz) mediated metal-free mild oxidation of thiols to disulfides in aqueous medium. *RSC Adv.* **6**, 39356–39363 (2016). <https://doi.org/10.1039/C6RA01509C>
  24. A. Ghorbani-Choghamarani, M. Hajjami, B. Tahmasbi, N. Noori, Boehmite silica sulfuric acid: as a new acidic material and reusable heterogeneous nanocatalyst for the various organic oxidation reactions. *J. Iran. Chem. Soc.* **13**, 2193–2202 (2016). <https://doi.org/10.1007/s13738-016-0937-4>
  25. D. Habibi, M.A. Zolfigol, M. Safaiee, A. Shamsian, A. Ghorbani-Choghamarani, Catalytic oxidation of sulfides to sulfoxides using sodium perborate and/or sodium percarbonate and silica sulfuric acid in the presence of KBr. *Catal. Commun.* **10**, 1257–1260 (2009). <https://doi.org/10.1016/j.catcom.2008.12.066>
  26. K.J. Liu, J.H. Deng, J. Yang, S.F. Gong, Y.W. Lin, J.Y. He, Z. Cao, W.M. He, Selective oxidation of (hetero)sulfides with molecular oxygen under clean conditions. *Green Chem.* **22**, 433–438 (2020). <https://doi.org/10.1039/c9gc03713f>
  27. M.A. Zolfigol, A. Khazaei, M. Safaiee, M. Mokhlesi, R. Rostamian, M. Bagheri, M. Shiri, H. Gerhardus Kruger, Application of silica vanadic acid as a heterogeneous, selective and highly reusable catalyst for oxidation of Sulfides at room temperature. *J. Mol. Catal. A: Chem.* **370**, 80–86 (2013). <https://doi.org/10.1016/j.molcata.2012.12.015>
  28. N. Noori, M. Nikoorazm, A. Ghorbani-Choghamarani, Oxovanadium immobilized on L-cysteine-modified MCM-41 as catalyst for the oxidation of sulfides and oxidative coupling of thiols. *Microporous Mesoporous Mater.* **234**, 166–175 (2016). <https://doi.org/10.1016/j.micromeso.2016.06.036>
  29. A. Bayat, M. Shakourian-Fard, M.M. Hashemi, Selective oxidation of sulfides to sulfoxides by a molybdate-based catalyst using 30% hydrogen peroxide. *Catal. Commun.* **52**, 16–21 (2014). <https://doi.org/10.1016/j.catcom.2014.03.026>
  30. Y.L. Hu, X.B. Liu, D. Fang, Efficient and convenient oxidation of sulfides to sulfones using H<sub>2</sub>O<sub>2</sub> catalyzed by V<sub>2</sub>O<sub>5</sub> in ionic liquid [C<sub>12</sub>mim][HSO<sub>4</sub>]. *Catal. Sci. Technol.* **4**, 38–42 (2014). <https://doi.org/10.1039/C3CY00719G>
  31. M. Nikoorazm, A. Ghorbani-Choghamarani, N. Noori, Preparation and characterization of functionalized Cu(II) Schiff base complex on mesoporous MCM-41 and its application as effective catalyst for the oxidation of sulfides and oxidative coupling of thiols. *J. Porous Mater.* **22**, 877–885 (2015). <https://doi.org/10.1007/s10934-015-9961-5>
  32. B. Atashkar, A. Rostami, H. Gholami, B. Tahmasbi, Magnetic nanoparticles Fe<sub>3</sub>O<sub>4</sub>-supported guanidine as an efficient nanocatalyst for the synthesis of 2H-indazolo[2,1-b]phthalazine-triones under solvent-free conditions. *Res. Chem. Intermed.* **41**, 3675–3681 (2015). <https://doi.org/10.1007/s11164-013-1480-x>
  33. B. Tahmasbi, A. Ghorbani-Choghamarani, First report of the direct supporting of palladium–arginine complex on boehmite nanoparticles and application in the synthesis of 5-substituted tetrazoles. *Appl. Organomet. Chem.* **31**, e3644 (2017). <https://doi.org/10.1002/aoc.3644>
  34. M. Nikoorazm, N. Noori, S. Faryadi, B. Tahmasbi, A palladium complex immobilized onto mesoporous silica: a highly efficient and reusable catalytic system for carbon–carbon bond formation and anilines synthesis. *Transit. Met. Chem.* **42**, 469–481 (2017). <https://doi.org/10.1007/s11243-017-0151-y>
  35. P. Moradi, M. Hajjami, B. Tahmasbi, Fabricated copper catalyst on biochar nanoparticles for the synthesis of tetrazoles as antimicrobial agents. *Polyhedron* **175**, 114169 (2020). <https://doi.org/10.1016/j.poly.2019.114169>
  36. L. Shiri, B. Tahmasbi, Tribromide ion immobilized on magnetic nanoparticles as an efficient catalyst for the rapid and chemoselective oxidation of sulfides to sulfoxides. *Phosphorus, Sulfur Silicon Relat. Elem.* **192**, 53–57 (2017). <https://doi.org/10.1080/10426507.2016.1224878>
  37. A. Ghorbani-Choghamarani, B. Tahmasbi, R.H.E. Hudson, A. Heidari, Supported organometallic palladium catalyst into mesoporous channels of magnetic MCM-41 nanoparticles for phosphine-free C–C coupling reactions. *Microporous Mesoporous Mater.* **284**, 366–377 (2019). <https://doi.org/10.1016/j.micromeso.2019.04.061>
  38. C. Han, Z. Li, W. Li, S. Chou, S. Dou, Controlled synthesis of copper telluride nanostructures for long-cycling anodes in lithium ion batteries. *J. Mater. Chem. A* **2**, 11683–11690 (2014). <https://doi.org/10.1039/C4TA01579G>
  39. Q. Li, S.W. Zhang, Y. Zhang, C. Chen, Magnetic properties in a partially oxidized nanocomposite of Cu–CuCl. *Nanotechnology* **17**, 4981 (2006). <https://doi.org/10.1088/0957-4484/17/19/034>
  40. M. Nikoorazm, A. Ghorbani-Choghamarani, A. Panahi, B. Tahmasbi, N. Noori, Pd(0)-Schiff-base@MCM-41 as high-efficient and reusable catalyst for C–C coupling reactions. *J. Iran. Chem. Soc.* **15**, 181–189 (2018). <https://doi.org/10.1007/s13738-017-1222-x>
  41. B. Tahmasbi, A. Ghorbani-Choghamarani, P. Moradi, Palladium fabricated on boehmite as an organic–inorganic hybrid nanocatalyst for C–C cross coupling and homoselective cycloaddition reactions. *New J. Chem.* **44**, 3717–3727 (2020). <https://doi.org/10.1039/c9nj06129k>
  42. A. Ghorbani-Choghamarani, P. Moradi, B. Tahmasbi, Modification of boehmite nanoparticles with Adenine for the immobilization of Cu(II) as organic–inorganic hybrid nanocatalyst in organic reactions. *Polyhedron* **163**, 98–107 (2019). <https://doi.org/10.1016/j.poly.2019.02.004>
  43. P. Moradi, M. Hajjami, F. Valizadeh-Kakhki, Biochar as heterogeneous support for immobilization of Pd as efficient and reusable biocatalyst in C–C coupling reactions. *Appl. Organomet. Chem.* **33**, e5205 (2019). <https://doi.org/10.1002/aoc.5205>
  44. M. Nikoorazm, Z. Rezaei, B. Tahmasbi, Two Schiff-base complexes of copper and zirconium oxide supported on mesoporous MCM-41 as an organic–inorganic hybrid catalysts in the chemo and homoselective oxidation of sulfides and synthesis

- of tetrazoles. *J. Porous Mater.* **27**, 671–689 (2020). <https://doi.org/10.1007/s10934-019-00835-6>
45. S. Hussain, D. Talukdar, S.K. Bharadwaj, M.K. Chaudhuri,  $\text{VO}_2\text{F}(\text{dmpz})_2$ : a new catalyst for selective oxidation of organic sulfides to sulfoxides with  $\text{H}_2\text{O}_2$ . *Tetrahedron Lett.* **53**, 6512–6515 (2012). <https://doi.org/10.1016/j.tetlet.2012.09.067>
46. X.F. Wu, A general and selective zinc-catalyzed oxidation of sulfides to sulfoxides. *Tetrahedron Lett.* **53**, 4328–4331 (2012). <https://doi.org/10.1016/j.tetlet.2012.06.003>
47. A. Shaabani, A.H. Rezayan, Silica sulfuric acid promoted selective oxidation of sulfides to sulfoxides or sulfones in the presence of aqueous  $\text{H}_2\text{O}_2$ . *Catal. Commun.* **8**, 1112–1116 (2007). <https://doi.org/10.1016/j.catcom.2006.10.033>
48. M. Hajjami, L. Shiri, A. Jahanbakhshi, Zirconium oxide complex-functionalized MCM-41 nanostructure: an efficient and reusable mesoporous catalyst for oxidation of sulfides and oxidative coupling of thiols using hydrogen peroxide. *Appl. Organomet. Chem.* **29**, 668–673 (2015). <https://doi.org/10.1002/aoc.3348>
49. S.M. Islam, A.S. Roy, P. Mondal, K. Tuhina, M. Mobarak, J. Mondal, Selective oxidation of sulfides and oxidative bromination of organic substrates catalyzed by polymer anchored Cu(II) complex. *Tetrahedron Lett.* **53**, 127–131 (2012). <https://doi.org/10.1016/j.tetlet.2011.10.138>
50. B. Karimi, D. Zareyee, Selective, metal-free oxidation of sulfides to sulfoxides Using 30% hydrogen peroxide catalyzed with N-bromosuccinimide (NBS) under neutral buffered reaction conditions. *J. Iran. Chem. Soc.* **5**, S103–S107 (2008). <https://doi.org/10.1007/BF03246497>
51. J. Zhang, T. Jiang, Y. Mai, X. Wang, J. Chen, B. Liao, Selective catalytic oxidation of sulfides to sulfoxides or sulfones over amorphous  $\text{Nb}_2\text{O}_5/\text{AC}$  catalysts in aqueous phase at room temperature. *Catal. Commun.* **127**, 10–14 (2019). <https://doi.org/10.1016/j.catcom.2019.04.013>
52. M. Safaiee, M. Moenimehr, M.A. Zolfigol, Pyridiniumporphyrinato oxo-vanadium tribromomethanide as a new source of  $\text{Br}^+$  catalyst for the chemo and homoselective oxidation of sulfides and benzylic alcohols. *Polyhedron* **170**, 138–150 (2019). <https://doi.org/10.1016/j.poly.2019.05.007>
53. A. Ghorbani-Choghamarani, M. Nikoorazm, H. Goudarziashar, B. Tahmasbi, An efficient and new method on the oxidative coupling of thiols under mild and heterogeneous conditions. *Bull. Korean Chem. Soc.* **40**, 1388–1390 (2009). <https://doi.org/10.1002/chin.200945034>
54. M. Hajjami, Z. Shirvandi, Z. Yousofvand, Zr(IV)-ninhydrin supported MCM-41 and MCM-48 as novel nanoreactor catalysts for the oxidation of sulfides to sulfoxides and thiols to disulfides. *J. Porous Mater.* **24**, 1461–1472 (2017). <https://doi.org/10.1007/s10934-017-0386-1>
55. M. Nikoorazm, A. Ghorbani-Choghamarani, H. Mahdavi, S.M. Esmaeili, Efficient oxidative coupling of thiols and oxidation of sulfides using UHP in the presence of Ni or Cd salen complexes immobilized on MCM-41 mesoporous as novel and recoverable nanocatalysts. *Microporous Mesoporous Mater.* **211**, 174–181 (2015). <https://doi.org/10.1016/j.micromeso.2015.03.011>